Bull. Res. Inst. Mar. Sci. & Tech.
Korea Maritime University.
Vol. 2. No. 1, p. 97-113.

Marine Structures 4 (1991) 257-273

Dynamics of Tension Leg Platform Tethers at Low Tension. Part I - Mathieu Stability at Large Parameters

M. H. Patel & H. I. Park

Santa-Fe Lab for Offshore Engineering, Department of Mechanical Engineering, University College London, Torrington Place, London WC1E 7JE, UK

(Received 5 November 1990; revised version received 3 January 1991; accepted 7 January 1991)

ABSTRACT

The tethers of tension leg platforms have conventionally been designed to have sufficiently high pre-tension so as not to go slack in extreme conditions of low tide levels and high waves. The high tether pre-tension necessary for this is found to be a significant restriction to the payload increase over conventional design that is needed for an operational platform. This paper reports on the first stage of an investigation into the dynamics of tethers with reduced pre-tension to facilitate payload increase over conventional design of a TLP.

When tether pre-tension is reduced, the wave-induced time-varying axial force becomes important in its dynamics. This time-varying axial force causes the tether to undergo parametric oscillations described by the Mathieu equation. Fortunately, in the case of a tether, even if it is in an unstable condition, the quadratic fluid damping force limits the amplitude of the lateral motion. However, the limited amplitudes vary according to the combination of the Mathieu parameters. Therefore, it is necessary to obtain the Mathieu stability chart up to the large parameters which can arise for tethers at low tension.

The governing partial differential equation is derived for lateral motion of a tether and reduced to the nonlinear Mathieu equation. The Mathieu stability chart is obtained over a wide range of parameters. In addition, the steady-state solutions of oscillation in the first instability region are obtained analytically. In order to obtain the solutions in higher-order instability regions, a numerical method is employed. The results show that even if tether is in a slack condition, the displacement amplitude of parametric oscillation is not

large for some dimensions. Therefore, it is possible to reduce the high pre-tension of tethers in terms at least of excitation of parametric tether oscillations.

Key words: TLP tether, low tension, time-varying axial force, parametric oscillations, Mathieu stability chart, peturbation technique, numerical method.

INTRODUCTION

As the shortage of oil and gas resources in shallow water becomes apparent, exploration and production of hydrocarbons is moving into deeper waters. The tension leg platform (TLP) is one of the most promising solutions for oil and gas production in deeper waters. The most significant design feature of a TLP is its tethers which are vertically connected to the sea bed and kept in high pre-tension by excess buoyancy in the platform. The design criterion for the pre-tension is based on the requirement that the tethers must not go slack in a hundred year extreme sea state coupled with low tide levels and high platform payload.

The principle of using pre-tension in vertical tethers provides a substantial advantage to a TLP in imparting a direct station-keeping property as well as very high natural periods in surge, sway and yaw and very low natural periods in heave, roll and pitch – both are designed to be well away from the normal periods of wave action. However, the consequent design penalty of high pre-tension is also a significant restriction to the payload increase over conventional design of a TLP. Therefore, the possibility of increasing payload over conventional design needs to be investigated further by examining the feasibility of reducing pre-tension in both existing and forthcoming TLP designs.

The pre-tension requirement of a TLP can be explored from two viewpoints. The first is re-consideration of environmental design considerations, which are believed to be currently too conservative.[1] For example, in the case of the Hutton TLP, the design environmental loads are assessed when all the extreme conditions of wind, current and tides occur simultaneously, which clearly has an extremely low probability of occurrence in reality. In addition, for extreme water level, the lowest design water level is taken as lower than LAT (the lowest astronomical tide). Therefore, a more complete probablistic approach to estimating loads due to combinations of environmental conditions is necessary for the payload increase over conventional design of TLPs. Such probability

considerations for TLPs must, of course, take account of the relatively greater importance of absolute sea levels for TLPs in comparison to other platforms.

The second line of enquiry needs to investigate the feasibility of adopting low tension tethers which would involve the tethers being adequately tensioned in normal sea states but going close to negative tension for short durations in a hundred year extreme sea state. This paper addresses this latter point and reports the first stage of an investigation into the dynamics of tethers with reduced pre-tension.

Some recent research work on TLP tethers is described below as background to the work presented in this paper. Harding and Banon[2] performed a reliability analysis to determine the adequacy of TLP tether maximum and minimum tension design criteria. Their results showed that the tether failure probability due to maximum tension (tension above yield) is much greater than that due to minimum tension (tension loss) when wave impact loads are included. This result suggests the possibility of tether tension reductions.

Brekke and Gardner[3] analysed the tether bending stress, platform motion and tether re-tensioning by a numerical simulation when tethers experience brief tension loss. They concluded that a brief period of tether tension loss does not lead to excess platform motion.

When a high pre-tension is reduced, the time-varying axial force acting on the tether becomes more important. Consideration of this force makes the governing equations of the tether itself and the surface platform become Mathieu type equations which describe parametric oscillations. In this first stage of work on low tether tensions, only the enhanced potential of a Mathieu stability of a tether is investigated.

Notable work has been carried out on the analysis of parametric oscillations of a long cylinder in water. Hsu[4] investigated the response of a parametrically excited hanging string in fluid. Stickland and Mason[5] analysed the importance of parametric oscillations on a TLP tether. This research showed that the hydrodynamic damping force plays an important role in limiting the response amplitudes of parametric oscillations. However, all of this work was confined to small magnitudes of the Mathieu equation parameters. In this case of TLPs, typical numerical values for such platforms lead to parameter values that are large and, therefore, it is necessary to investigate the Mathieu equation over a large parameter range.

In this paper the governing partial differential equation of tether lateral motion is reduced to the nonlinear Mathieu equation by applying Galerkin's method and the method of separation of variables. The Mathieu chart for large value parameters is obtained followed by the

steady-state solution of a parametric oscillation in the first instability region using a perturbation method. Due to the large magnitude of parameters, a fourth-order Runge-Kutta method is employed to obtain the phase plane and time history of tether motions.

GOVERNING EQUATION OF TETHER LATERAL MOTION

The tether of a TLP is considered as a straight, simply supported column of uniform cross section as shown in Fig. 1. The tether is subjected to a time varying axial force exerted by the platform with wave and current forces on the tether neglected. Using simple beam theory and neglecting axial inertia, the governing equation of lateral motion can be written as:

$$M\frac{\partial^2 y}{\partial t^2} + EI\frac{\partial^4 y}{\partial x^4} - \frac{\partial}{\partial x}\left\{(P - S\cos\omega t)\frac{\partial y}{\partial x}\right\} + B_v\left|\frac{\partial y}{\partial t}\right|\frac{\partial y}{\partial t} = 0 \qquad (1)$$

where M is the sum of physical and added masses per unit length of the tether, EI is the tether flexural rigidity, P is axial tension, S is the imposed axial force amplitude, ω is the wave frequency and B_v is the quadratic

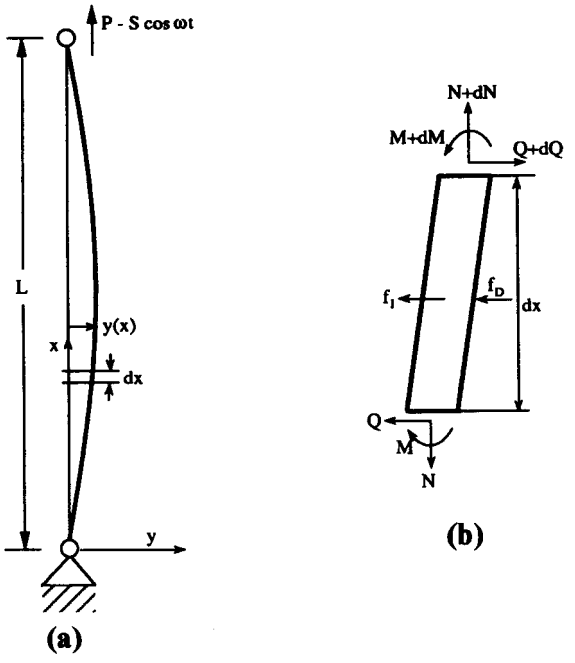

Fig. 1. (a) Tether model configuration; (b) element notation.

fluid damping coefficient. Here the wave-induced axial force, $S\cos\omega t$, is assumed to be sinusoidal. The assumption is based on the fact that even if ocean waves are irregular, the time-varying axial forces become more regular (that is a more narrow banded spectrum) due to the transfer function from wave action to tether forces. In addition, the possibility of slackening of low tension tethers is rather greater in large long period waves which tend to be more narrow banded in spectral content.

Taking the fundamental mode (the largest amplitude mode of the model) only and using the method of separation of variables, the solution of eqn (1) can be written in the form:

$$y(x,t) = f(t)\sin\frac{\pi x}{L} \tag{2}$$

where L is the total length of the tether. The analysis for high modes also needs to be carried out since these are active in the coupling between platform and tether dynamics. However, these high modes have not been considered here for brevity.

To find the unknown deflection $f(t)$, the Galerkin variational method is used. Substituting eqn (2) into eqn (1), multiplying it by $\sin(\pi x/L)$ and integrating with respect to x between 0 and L, gives the following equation:

$$\frac{\mathrm{d}^2 f}{\mathrm{d}t^2} + \left(\frac{EI\pi^4}{ML^4} + \frac{P\pi^2}{ML^2} - \frac{S\pi^2}{ML^2}\cos\omega t\right) f + \frac{8B_v}{3\pi M}\left|\frac{\mathrm{d}f}{\mathrm{d}t}\right|\frac{\mathrm{d}f}{\mathrm{d}t} = 0 \tag{3}$$

using the following integrals

$$\int_0^L \sin^2\frac{\pi x}{L}\,\mathrm{d}x = \frac{L}{2} \quad \int_0^L \sin^3\frac{\pi x}{L}\,\mathrm{d}x = \frac{4L}{3\pi}$$

From eqn (3), it can be seen that if tether length is long, the bending stiffness force is very small compared to pre-tension and can be neglected. However, for slightly loaded and/or short structures, the bending stiffness force plays an important role in parametric oscillations.

It is convenient to introduce a dimensionless time variable, τ, such that:

$$2\tau = \omega t, \quad \text{then} \quad \frac{\mathrm{d}^2 f}{\mathrm{d}t^2} = \frac{\omega^2}{4}\frac{\mathrm{d}^2 f}{\mathrm{d}\tau^2} \tag{4}$$

Substituting eqn (4) into eqn (3) gives the final equation:

$$\frac{\mathrm{d}^2 f}{\mathrm{d}\tau^2} + (\delta - 2q\cos 2\tau)f + c\left|\frac{\mathrm{d}f}{\mathrm{d}\tau}\right|\frac{\mathrm{d}f}{\mathrm{d}\tau} = 0 \tag{5}$$

where:

$$\delta = \frac{(2\bar{\omega})^2}{\omega^2} \qquad q = \frac{2S\bar{\omega}^2}{P\omega^2} \qquad c = \frac{8B_v}{3\pi M} \qquad \bar{\omega} = \frac{\pi}{L}\sqrt{\frac{P}{M}}$$

and $\bar{\omega}$ is the frequency of the first mode of free vibration of a loaded tether. Equation (5) is the nonlinear Mathieu equation which describes a parametrically excited system. The Mathieu equation has some particular characteristics - its solution becomes stable or unstable according to the combination of the parameter of δ and q. However, if a nonlinear damping term is included as in eqn (5), even the unstable solutions become limited in amplitude. If the nonlinear damping term is linearised, the stability areas of the Mathieu chart increase but unstable areas remain. This leads to the two results becoming quite different from each other and therefore linearisation cannot be carried out in the parametric oscillation case. So far previous research into the Mathieu equation has been carried out for small magnitudes of δ and q. However, in the case of the tethers of TLPs or rigid risers, numerical values of δ and q can be very large up to 300 for δ and 150 for q in metric units. It is therefore necessary to obtain the Mathieu stability chart for these large parameters.

MATHIEU STABILITY CHART FOR WIDE RANGE OF PARAMETERS

A canonical form of the Mathieu equations takes its form by excluding the nonlinear damping term of eqn (5), i.e.

$$\frac{d^2f}{d\tau^2} + (\delta - 2q\cos 2\tau)f = 0 \tag{6}$$

A particular characteristic of the Mathieu equation is that it contains a periodically varying coefficient as a special case of the Hill equation. This means that the solutions of the Mathieu equation can be stable or unstable according to the combination of δ and q. Thus the approach to the Mathieu equation is to obtain a general solution like other differential equations and a stability chart which shows whether the system is in a stable or unstable condition. In this analysis, the stability chart is obtained with the nonlinear damping term excluded.

For small magnitude parameters, a stability chart already exists as reported by Ince[6] and Goldstein[7]. Based on Goldstein's approach, the stability chart up to large parameters is obtained as follows.

It is known that when δ of eqn (6) belongs to a certain countable set of characteristic values, eqn (6) is satisfied by one of the following periodic solutions:

$$f = \sum_{n=0}^{\infty} A_{2n} \cos 2n\tau \quad \text{(Even solution of period } \pi\text{)}$$

$$f = \sum_{n=0}^{\infty} A_{2n+1} \cos (2n+1)\tau \quad \text{(Even solution of period } 2\pi\text{)}$$

$$f = \sum_{n=0}^{\infty} B_{2n+1} \sin (2n+1)\tau \quad \text{(Odd solution of period } \pi\text{)}$$

$$f = \sum_{n=0}^{\infty} B_{2n+2} \sin (2n+2)\tau \quad \text{(Odd solution of period } 2\pi\text{)} \qquad (7)$$

If the above series are substituted in turn into eqn (6) and the coefficients of $\cos (2n\tau)$, $\cos (2n+1)\tau$, $\sin (2n+1)\tau$ and $\sin (2n+2)\tau$ are equated to zero for $n = 0, 1, 2 \ldots$, recurrence relations are obtained. With some manipulation, these recurrence relations can be expressed into infinite and terminated continued fractions. In order for the recurrence relations to be consistent, two continued fractions must be equal. By using a trial and error method, and inter- and extrapolation methods, satisfiable δ values can be obtained for given n and q values.

Following the above procedure, a computer program was developed to obtain tabulated values of δ and q for $n = 1, 2, \ldots$. In this paper, the values of δ and q are calculated up to 280 and 140, respectively. The computing time to calculate these large values of δ and q takes less than 1 min on a Digital Equipment Corporation Micro VAX-II computer. The tabulated values are plotted in Fig. 2 which is called the Mathieu stability chart or the Ince–Strutt chart.

For small values of δ and q, the results obtained in this work are in agreement with conventional exact results. However, there is no such information in the research literature for large values of δ and q. Thus the Mathieu eqn (6) is solved numerically using the fourth-order Runge-Kutta method to check that the solution is stable in stable regions or unstable in unstable regions. One result for the ninth instability region is shown in Fig. 3. The response amplitudes, f, are the values of numerical calculation at non-dimensional time $\tau = 100$. As can be seen from Fig. 3(b), in the unstable range, $\delta = 98$ to 102, the response amplitudes are very high but in the adjacent stable regions, the amplitudes are zero. This Mathieu stability chart was also verified for other regions of instability at high values of q.

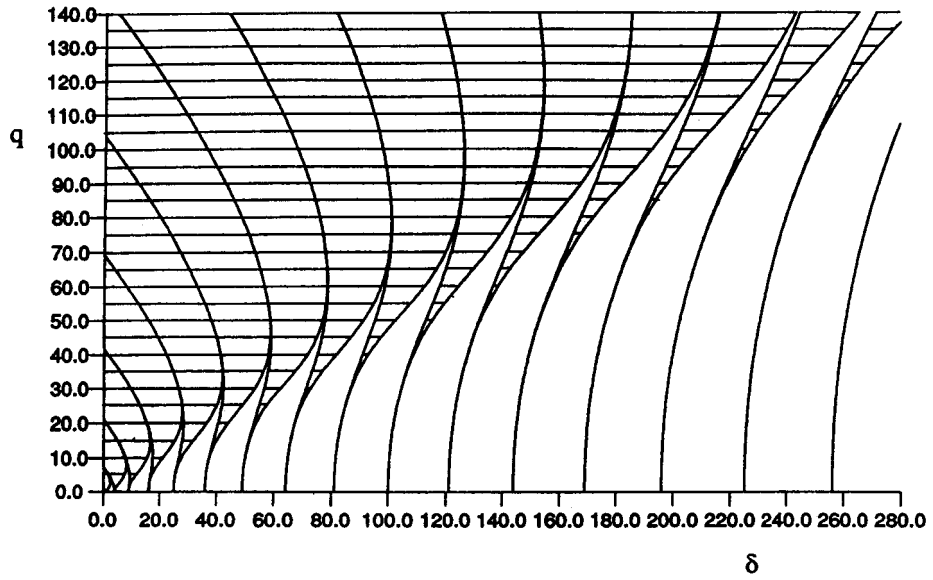

Fig. 2. Mathieu stability chart up to large parameters (shade regions are unstable).

It is useful to apply the chart to TLP tethers. Figure 4 shows how the stability condition of an example tether taken from the Hutton TLP platform varies with its characteristics of tether length, pre-tension and wave induced force amplitude. The straight line OA in Fig. 4 denotes a boundary between slack and tensioned tether conditions. In other words $q - \delta$ values for a slack tether plot above OA whereas those for a tensioned tether plot below OA. It can be observed that this boundary line passes alternately through stable and unstable regions of the Mathieu chart. Point B shows the present normal operating condition of

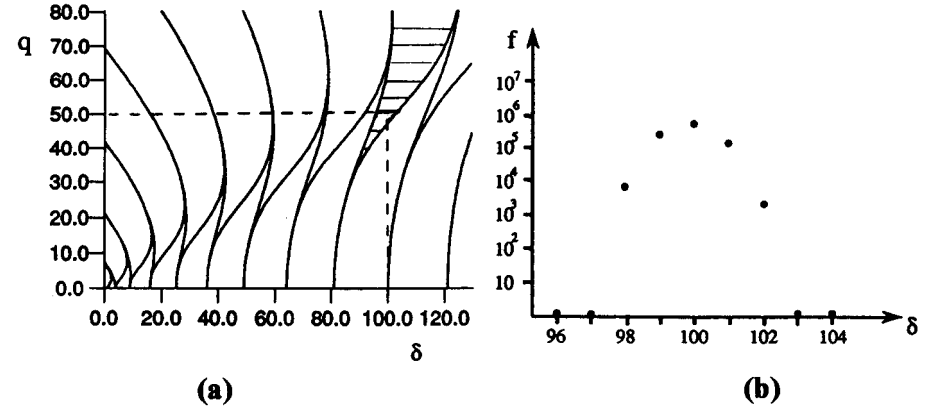

Fig. 3. Examination of the Mathieu stability chart. (a) Ninth instability region; (b) response amplitude at $q = 50$.

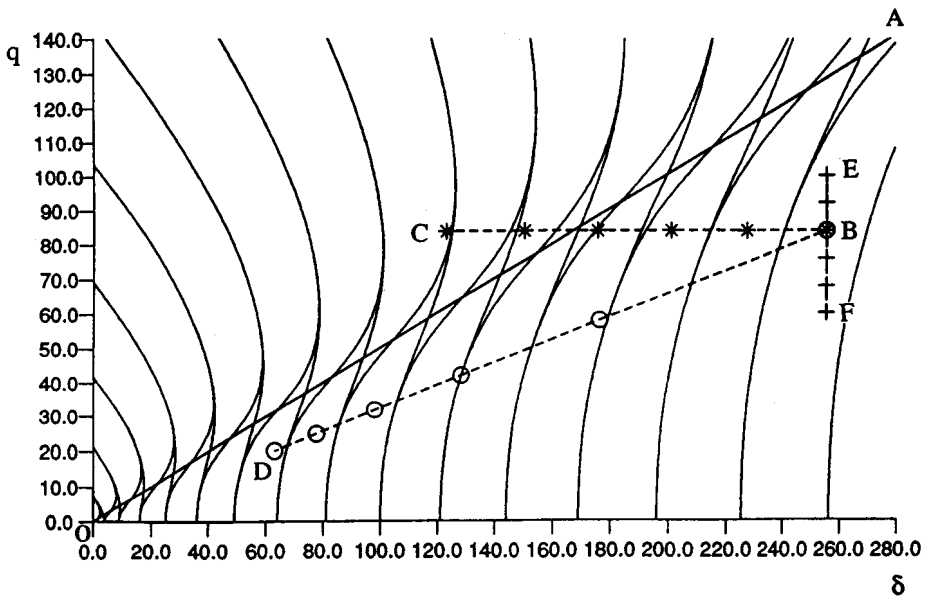

Fig. 4. Behaviour of stability condition for the Hutton TLP Tether. +, Amplitude of axial force variation; ⊖, tether length; ⊛, present condition; *, pre-tension; ———, transition line.

a tether of the Hutton TLP. If the pre-tension of this tether was reduced, the operating point B would shift towards C and encounter the first unstable region at a value of δ of approximately 190. Line BD denotes movement of the operating point for increasing tether length (or water depth) whereas lines EBF indicate the variation of operating point due to changes in the amplitude of axial force variation.

While constructing the Mathieu chart, the damping term was not considered. In reality, in the tether case, the nonlinear hydrodynamic damping force plays an important role in limiting tether oscillations. So, even if a tether is in an unstable condition, the response amplitude will be limited due to the nonlinear damping force. This feature is investigated below. It is noted that if a system corresponds to a stable condition, the response amplitude becomes zero and so the following approaches are carried out only for unstable regions of the Mathieu chart.

PERTURBATION METHOD TO SOLVE THE NONLINEAR MATHIEU EQUATION FOR SMALL PARAMETERS

Perturbation methods are usually employed to analytically solve a nonlinear differential equation. Some research workers have used the method for the nonlinear Mathieu equation with a quadratic damping

term and/or a cubic displacement term (Hsu[8], Nayfeh,[9]). Perturbation methods are, however, confined to small parameters but very useful to identify the global pattern of solutions.

Of the perturbation techniques, the averaging method is employed in this work to solve the nonlinear Mathieu equation, eqn (5). The solution is considered only to a first approximation. Following the averaging method (see e.g. Minorsky[10] for further details), the solution is obtained as:

$$f = \hat{a}\cos(\tau + \hat{\theta}) - \left(\frac{\hat{a}q}{8}\right)\{\cos 2\hat{\theta}\cos 3(\tau + \hat{\theta}) + \sin 2\hat{\theta}\cos 3(\tau + \hat{\theta})\}$$

$$+ \hat{a}^2 c \sum_{m}^{\infty} \frac{8}{\pi m(m^2 - 4)} \sin m(\tau + \hat{\theta}) \qquad m = 5,7,9,..... \tag{8}$$

$$\text{where: } \hat{a} = \frac{3\pi}{8c}\sqrt{q^2 - (\delta - 1)^2} \tag{9}$$

$$\hat{\theta} = \frac{1}{2}\sin^{-1} - \sqrt{1 - \frac{(\delta - 1)^2}{q^2}} \tag{10}$$

The above result is related to the first instability region of the Mathieu chart and provides important information for the nonlinear Mathieu equation with a quadratic damping term. As can be seen from eqn (9), the response amplitudes are limited even if a system is in the instability region. Substituting eqn (8) into eqn (2) gives a complete solution of parametric tether oscillations in a condition corresponding to the first instability of the Mathieu chart. One important result is the steady-state response amplitude, $\hat{a}$, plotted against δ and q in Fig. 5. At $\delta = 1$, i.e. at the centre of the instability region, $\hat{a}$ has its maximum value:

$$\hat{a}_m = \frac{3\pi}{8c}q \tag{11}$$

It can be seen that $\hat{a}_m$ is proportional to the strength of the parametric oscillation, q and inversely proportional to the damping coefficient, c.

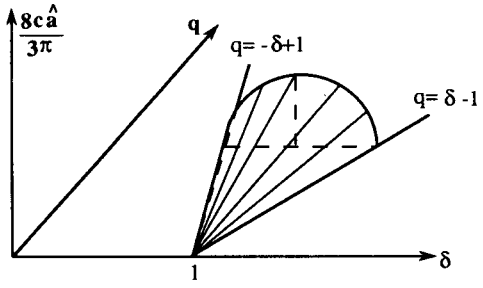

Fig. 5. Stationary amplitude of the nonlinear Mathieu equation in the first instability region.

Equation (11) can be expressed in terms of tether characteristics from eqn (5).

$$\text{At } \bar{\omega} = \frac{\omega}{2}, \quad \hat{a}_{\max} = \frac{9\pi^2 MS}{128 B_v P} \tag{12}$$

Equation (12) indicates that maximum response amplitudes occur when the external frequency is twice the natural frequency. It should be noted that the above result is applicable to the first instability region only. It is also possible to obtain analytically the steady-state solution for the second and higher order instability regions. However, second and higher order approximations are needed and the calculation becomes very complicated. Therefore, the nonlinear Mathieu equation with large magnitude parameters needs to be solved to take this investigation further. This can only be done using a numerical method.

NUMERICAL METHOD

Of the numerical methods for ordinary differential equations, the fourth-order Runge-Kutta method is widely used due to its stability and accuracy. In this analysis the Runge-Kutta method is employed to obtain the solution of the nonlinear Mathieu equation, eqn (5), with large parameters. As can be seen from the previous analytical result, eqn (9), the response also depends on the value of damping coefficient, c. Since this work is focused on the relative importance of various conditions under which parametric oscillations can occur, it was decided to adopt a value of c of 0·3 for those calculations. This value was chosen to be mid-way between a typical range of from 0·2 to 0·4 for the coefficient of a TLP tether. The initial conditions for the numerical solution do not influence the steady-state solution of the nonlinear Mathieu equation and the initial conditions $f(0) = 0$, $\mathrm{d}f(0)/\mathrm{d}\tau = 1{\cdot}0$ are used. Equation (5) is then solved numerically for different values of parameters, δ and q. Numerical results for the first instability region are compared with the analytical result from eqn (11). There is close agreement between the two as shown by Fig. 6.

Phase planes and time histories of generalised displacements are then computed for different tether conditions; that is, tensioned, transitional and slack conditions. These conditions are illustrated in Fig. 7. For these three conditions, phase plane and time histories of generalised displacements of the first, third and ninth instability regions are plotted in Figs 8, 9 and 10, respectively, where the overdot denotes differentiation

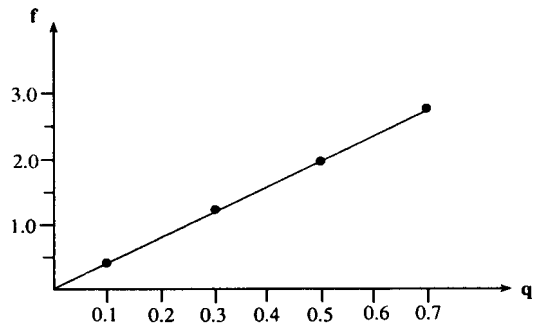

Fig. 6. Comparison of stationary amplitudes in the centre of the first instability region between numerical (●) and analytical (——) results.

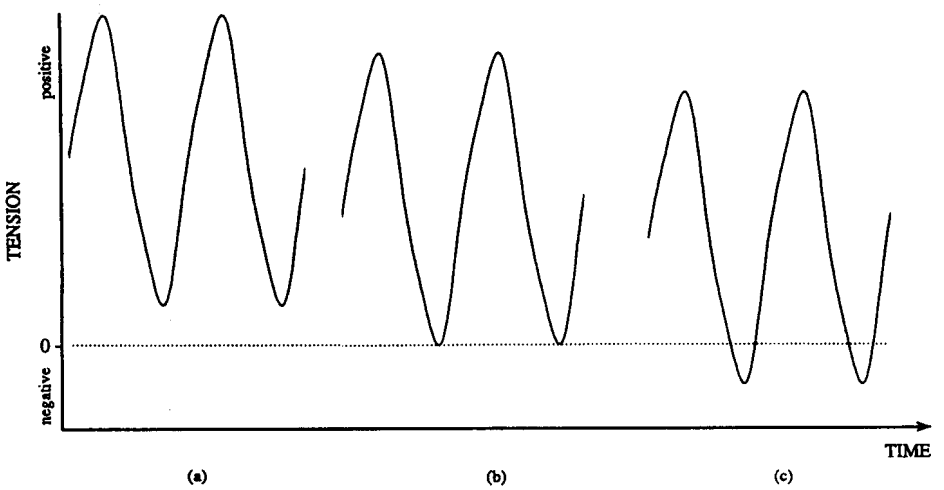

Fig. 7. Illustration of tether tension condition. (a) Tension; (b) transitional; (c) slack.

with respect to τ. These figures can be expressed in terms of tether conditions as follows:

Figs 8(a), 9(a) and 10(a) - Tension conditions
Figs 8(b), 9(b) and 10(b) - Transitional conditions between tensioned and slack
Figs 8(c), 9(c) and 10(c) - Slack conditions

Figures 8, 9 and 10 give results for conditions at the centre of their respective regions of instability; that is, they give the largest amplitude for the same value of q. As can be seen from the figures, the response amplitudes reduce gradually as the order of instability increases. For tensioned tethers, the responses are small even in the first region of instability. In the transitional condition, when the pre-tension is equal to the force amplitude, tether amplitudes are large in the first region of

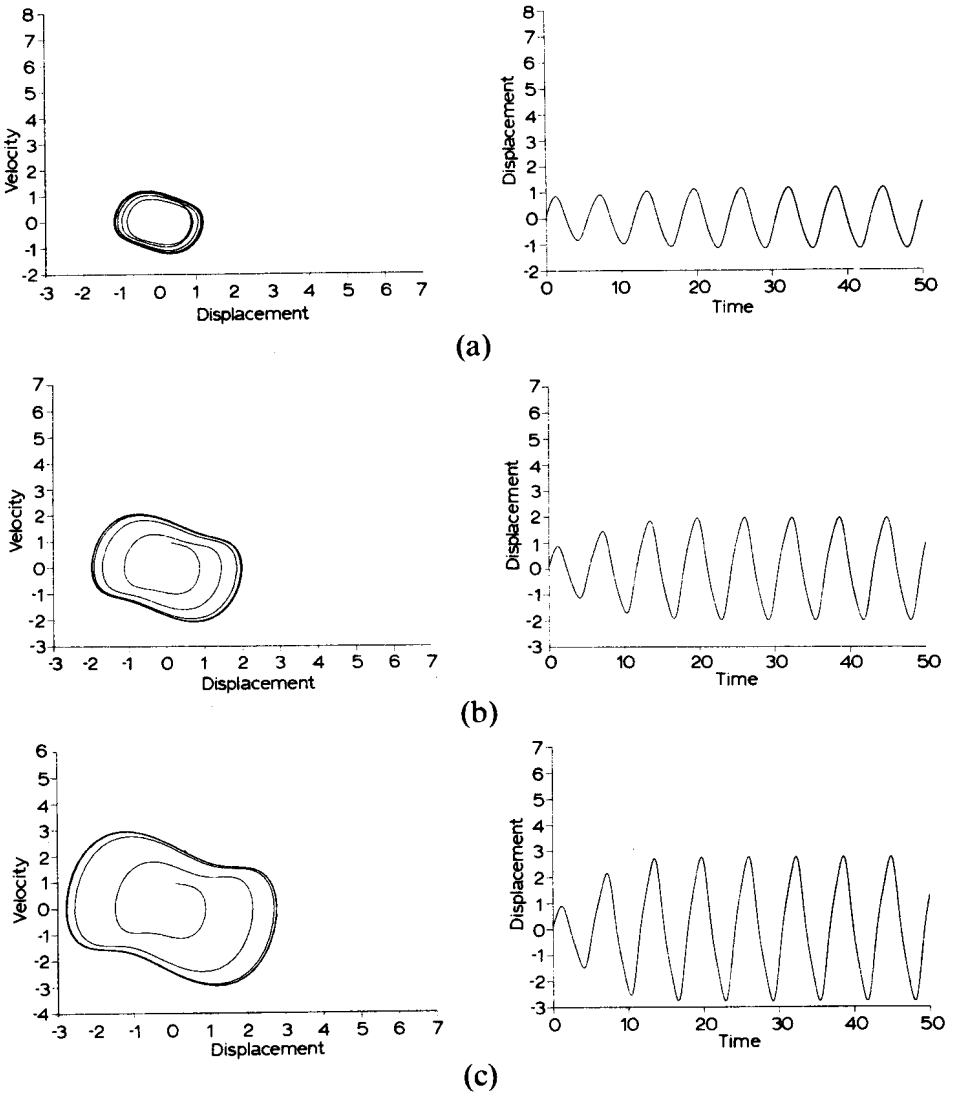

Fig. 8. Phase plane and time history of a generalised displacement in the first instability region for (a) $\delta = 1{\cdot}0$, $q = 0{\cdot}3$ (tensioned condition); (b) $\delta = 1{\cdot}0$, $q = 0{\cdot}5$ (transitional condition); (c) $\delta = 1{\cdot}0$, $q = 0{\cdot}7$ (slack condition).

instability. In metric units, the total displacement amplitude in the first region of instability is 4 m. However, in higher order instability regions, the responses are very small. It is clear from these results that the Mathieu instability for low tension tethers is significant in lower order instability regions. This, in fact, corresponds to numerical values for tethers in deeper water. It should be noted that here time is non-dimensionalised using eqn (4). So for a particular tether, the time

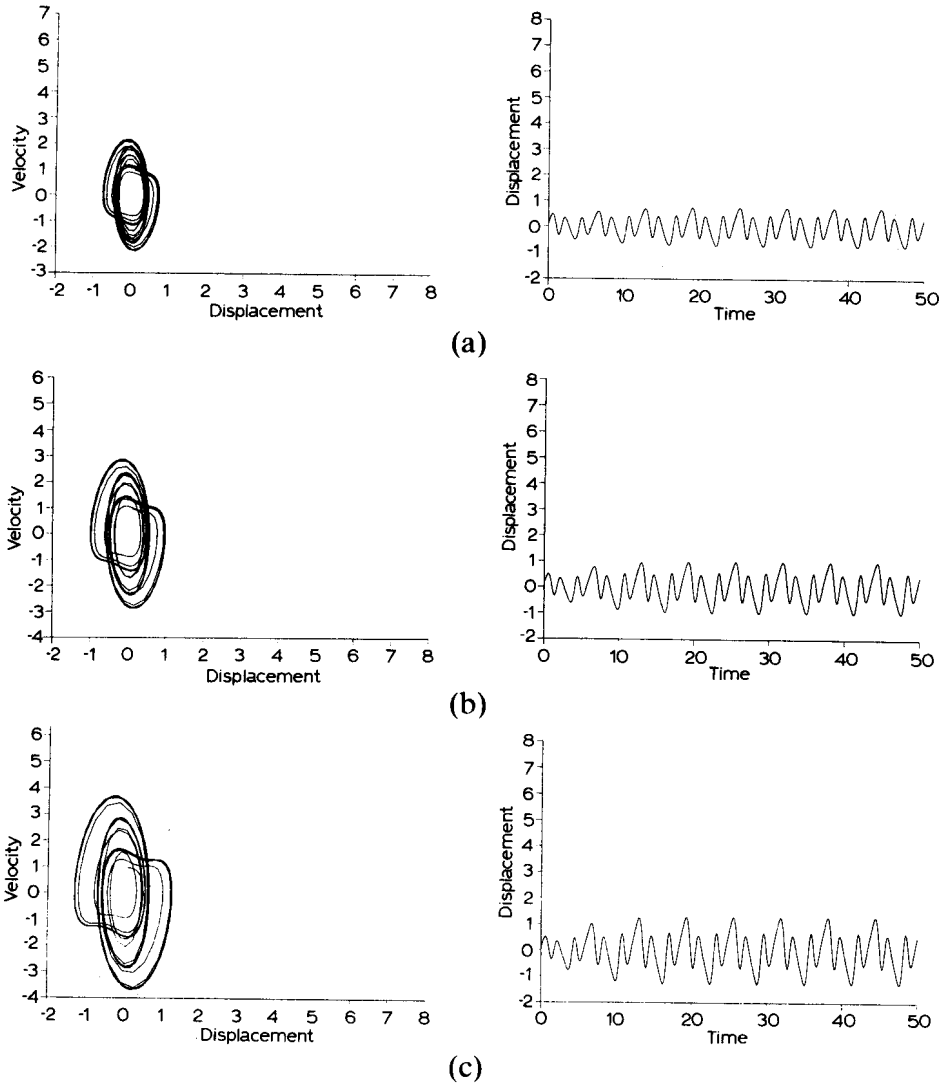

Fig. 9. Phase plane and time history of a generalised displacement in the third instability region for (a) $\delta = 10{\cdot}25$, $q = 4{\cdot}75$ (tensioned condition); (b) $\delta = 10{\cdot}5$, $q = 5{\cdot}25$ (transitional condition); (c) $\delta = 10{\cdot}75$, $q = 5{\cdot}75$ (slack condition).

histories and the velocities of the phase plane should be dimensionalised by using wave frequency ω.

Since this research is aimed at the potential of the Mathieu instability of tethers at low tension, particular emphasis is placed on the zero tension slack condition. Even if the tether is in a slack condition, all the response amplitudes in the stable regions of the Mathieu chart become zero. Therefore, in terms of parametric oscillation, slack tethers can be

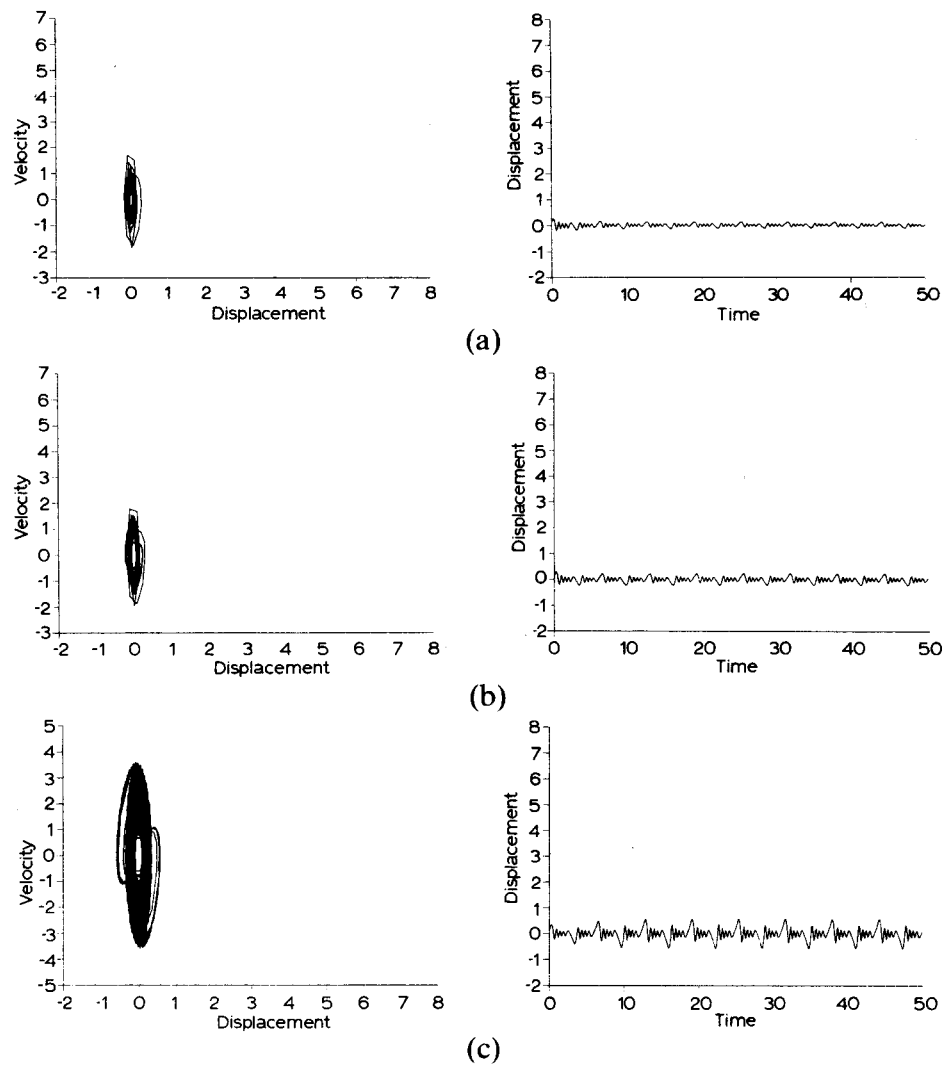

Fig. 10. Phase plane and time history of a generalised displacement in the ninth instability region for (a) $\delta = 98{\cdot}0$, $q = 47{\cdot}5$ (tensioned condition); (b) $\delta = 100{\cdot}0$, $q = 50{\cdot}0$ (transitional condition); (c) $\delta = 103{\cdot}0$, $q = 55{\cdot}0$ (slack condition).

undoubtedly adopted in stable regions. However, in unstable regions, as can be seen from Figs 8(c) and 9(c), the maximum response amplitudes are somewhat larger in lower-order instability regions and these magnitudes might not be permissible for an operational TLP. In higher-order instability regions like Fig. 10(c), the maximum response amplitude is small and can be permissible. By using the Mathieu chart obtained here, the relative magnitude of response amplitudes of parametrically oscillating tethers can be usefully determined for slack tether cases.

As can be known from the above, the parametric oscillation is important only in lower-order instability regions. Although in this work, tether axial forces have been assumed to be regular, the random nature of actual wave forces can cause the Mathieu instability to be less dominant. However, there are two aspects of the problem which still require the Mathieu instability in regular waves to be examined. The first is that despite irregular incident waves, the inertia of a TLP can cause the resultant tether axial forces to tend towards near sinusoidal oscillations. A further reason for this study is that the Mathieu instability requires to be examined in conditions of low tether tension.

It is often argued that if tethers go slack, the phenomenon of snap or snatch loading of the tethers occurs. For example, when a towboat re-tensions a slack cable, the snatch loading can be serious due to a significant relative velocity between the ends of the cable. However, in the case of tethers, the considered tension loss is not large enough and the surface platform does not acquire the large velocity required for significant snatch loading. The hydrodynamic drag force also plays an important role in protecting against the adverse effects of snatch loading. However, further research into snatch loading of slack tethers is necessary and is being examined in later aspects of this work.

In this study, it has been assumed that the top ends of tethers do not move in the horizontal direction. However, if the horizontal motion is also considered, the motion of tethers becomes combined forced and parametric oscillations, which is very complicated to solve analytically. The combined oscillations and the interaction between the surface platform and tether dynamics at low tension is being investigated and will be presented in future work.

CONCLUSION

This paper quantifies the enhanced potential of Mathieu stability in tethers with reduced pre-tension. This is studied as the first stage of an investigation into the dynamics of low tension tethers to facilitate payload increase over conventional design of a TLP. The Mathieu stability chart up to large parameters is obtained and justified. Even for tether operating in an unstable condition, their response amplitude is limited due to hydrodynamic fluid damping force but the response magnitudes vary according to the Mathieu parameters.

The response amplitudes of the tether in any condition (slack, transitional or tensioned) increase as the instability region moves to lower orders, which corresponds to deeper water tethers. Therefore, the

Mathieu type instability problem is more significant for deep water TLP designs. In the slack tether case considered here, the maximum response amplitude is zero in the stable regions and small enough to be acceptable in the higher order instability regions but somewhat large in the lower order instability regions.

Thus the Mathieu stability chart prescribed in this paper can be used to guide design work aimed at reducing the mean pre-tension of TLPs as an aid to payload increase over conventional design of a TLP. However, further work needs to be carried out to examine the combined parametric and forced oscillation of tethers as well as the coupling between the surface platform and tethers dynamics at low pre-tension.

REFERENCES

1. Mercier, J. A., Evolution of Hutton TLP response to environmental loads *OTC 4429*, (1982).
2. Harding, S. J. & Banon, H., Reliability of TLP tethers under maximum and minimum life time loads, *OTC 5935*, (1989).
3. Brekke, J. N. & Gardner, T. N., Analysis of brief tension loss in TLP tethers, *Journal of Offshore Mechanics and Arctic Engineering*, **110** (February, 1988) 43–7.
4. Hsu, C. S., The response of a parametrically excited hanging string in fluid, *Journal of Sound and Vibration*, **39**(3), (1975), 305–16.
5. Strickland, G. E. & Mason, A. B., Parametric response of TLP tendons — Theoretical and numerical analysis, *OTC 4071* (1981).
6. Ince, E. L., Researches into the characteristic numbers of the Mathieu equation, *Proc. Royal Society of Edinburgh*, **46** (1925) 20–9.
7. Goldstein, S., Mathieu functions, *Trans. Cambridge Philosophical Society*, **23** (1929) 303–36.
8. Hsu, C. S., Limit cycle oscillations of parametrically excited second-order nonlinear systems, *Journal of Applied Mechanics*, (March 1975), 176–82.
9. Nayfeh, A. H., *Introduction to Perturbation Techniques*, John Wiley and Sons, New York, 1981.
10. Minorsky, N., *Nonlinear Oscillations*, Van Nostrand Company, Princeton, NY, 1962.